

2000; Redaelli and Macek, 2001), correlation dimension (Macek and Obojska, 1997; Gupta *et al.*, 2008) and Lyapunov exponents (Macek and Obojska, 1998; Redaelli and Macek, 2001; Gupta *et al.*, 2008) show that solar wind velocity fluctuations are a consequence of complex nonlinear dynamical processes. Inherent changes in the dynamics governing the solar wind velocity at 0.3 AU have been observed (Gupta *et al.*, 2008). Milano *et al.* (2004) analyzed magnetic and bulk velocities measured by ACE and found an anisotropy in the velocity, magnetic, and cross helicity correlation functions and power spectra. McComas, Gosling, and Skoug (2000) analyzed Ulysses observations to demonstrate that the mid-latitude solar wind structure becomes increasingly complex as solar activity increases. Consolini, Tozzi, and de Michelis (2009) investigated the emergence of spatio-temporal complexity in the 11-year solar cycle monitored by sunspot activity. They showed that spatio-temporal or dynamical complexity is an intrinsic property of the solar cycle. Using information entropy approach to the sunspot number time series, they showed how the dynamical complexity increases during the maximum phase of the solar cycle.

Hysteresis occurs in several phenomena in physics, chemistry, biology, and engineering. It is a nonlinear phenomenon observed in systems from diverse areas of science, *e.g.*, electromagnetism, electro-plasticity, superconductivity, and granular motion (Bertotti, 1998; Guyer, TenCate, and Johnson, 1999; Katzgraber *et al.*, 2002; Zharkov, 2002). This phenomenon occurs when a nonlinear system has at least two coexisting stable states in the hysteresis region where the system is found to depend on the history of the dynamics. Here, in dynamical systems, history corresponds to the system's initial conditions. For example, hysteresis is observed in van der Pol system, Duffing system (Thompson and Stewart, 1986), and Lorenz system (Alfsen and Frøyland, 1985). The hysteresis has been observed in coupled nonlinear systems as well (Prasad *et al.*, 2005).

Hysteresis phenomenon has been noticed in various solar indices. Bachmann and White (1994) observed the presence of hysteresis patterns among many pairs of activity indices during solar cycle 21 and 22. They found that this hysteresis can be expressed approximately as a hierarchy of delay times behind the leading index, the sunspot number. Jiménez-Reyes *et al.* (1998) analyzed the low-degree p -mode frequency shifts and solar activity indices (radio flux at 10.7 cm and magnetic index) over solar cycle 22 and observed a hysteresis phenomenon. Moreno-Insertis and Solanki (2000) suggested that high latitude fields are necessary to produce a significant difference in hysteresis between odd and even-degree p -modes frequencies. Tripathy *et al.* (2000) reported that the intermediate degree p -mode frequencies of solar cycle 22 show a hysteresis phenomenon with the magnetic indices whereas no such effect exists for the radiative indices. Özgüç and Ataç (2001) showed the presence of hysteresis between the solar flare index and some solar activity indicators such as total sunspot area, mean magnetic field, and coronal index during solar cycles 21 and 22. They found that these indices follow different paths for ascending and descending phases of the solar cycles while saturation effect exists at the extreme phases.

In the present work, we attempt to understand the dynamics of ascending and descending phases of a solar cycle. We use permutation entropy (S) of hourly averaged solar wind velocity time series to capture the complexity trend over a cycle. We use the data obtained from ACE during 1998 – 2010. This period

belongs to solar activity cycle 23. We use permutation entropy (S) to detect the hysteresis in a dynamical system and calculate it for time series obtained from simulated as well as solar wind velocity data.

In the next section, we review the algorithm to calculate the permutation entropy (S) of a time series. In Section 3 we describe how S detects the multistability present in the modeled dynamical system. In Section 4 we analyze solar wind data using permutation entropy. This is followed by conclusions in Section 5.

2. Permutation Entropy

Lyapunov exponent, entropy, and fractal dimension are well known and extensively used measures to detect dynamical changes in a time series obtained from a complex system (Kantz and Schreiber, 2004). Calculation of these quantities needs phase space reconstruction for which we need to know the parameters like embedding dimension and delay (Packard *et al.*, 1980). However, in practice, it is very difficult to get accurate parameters, particularly for noisy data. Permutation entropy can be used to compare two or more time series and distinguish regular, chaotic and random behavior for small and noisy time series (Bandt and Pompe, 2002). It quantifies not the only randomness but also the degree of correlational structures of a time series (Rosso *et al.*, 2007). Permutation entropy is conceptually simple and computationally very fast (Cao *et al.*, 2004). It can be effectively used to detect dynamical changes in a complex system. The detailed algorithm to calculate permutation entropy is described below :

Let us consider a time series $x_i, i = 1, 2, \dots, N$ and embed it in an m -dimensional space (Packard *et al.*, 1980). An embedded vector is written as

$$X_i = [x_i, x_{i+1}, \dots, x_{i+(m-1)}].$$

For each embedded vector X_i , the m components can be arranged in an increasing order: $[x_{i+k_1} < x_{i+k_2} < \dots < x_{i+k_m}]$, where k_j can have any value from 0 to $m-1$. Hence, each vector X_i is uniquely mapped onto (k_1, k_2, \dots, k_m) which is one of the $m!$ permutations of m distinct symbols $(0, 1, \dots, m-1)$. When each permutation is considered as a symbol, the reconstructed trajectory in the m -dimensional space is represented by a symbol sequence. We denote the probability distribution for the distinct symbol by P_1, P_2, \dots, P_j , where $j \leq m!$. The permutation entropy for the time series $x_i, i = 1, 2, \dots, N$ is defined (Bandt and Pompe, 2002) as the Shannon entropy for the j distinct symbols

$$S(m) = - \sum_{j=1}^{m!} P_j \ln(P_j). \quad (1)$$

Here $S(m)$ attains the maximum value $\ln(m!)$ when $P_j = \frac{1}{m!} \forall j$; for uniformly distributed data. Therefore, normalized permutation entropy is written as

$$S = \frac{S(m)}{\ln(m!)}, \quad (2)$$

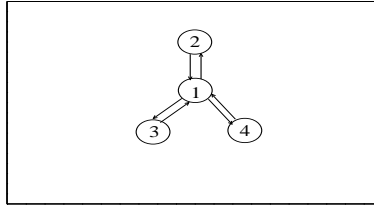


Figure 1. Schematic configuration of coupled oscillators represented by Equation (3).

where the value of S lies between 0 and 1. Smaller value of S indicates a more regular time series. If m is too small there are very few distinct states and this scheme will not work. A value of $m = 5, 6$, or 7 is suitable to calculate the permutation entropy for detecting the dynamical changes in a system (Bandt and Pompe, 2002; Cao *et al.*, 2004).

3. Dynamical Hysteresis

Hysteresis occurs when a nonlinear system has at least two existing stable states in a hysteresis region. Out of multiple states, the system attains a state depending on the history of the dynamics, *e.g.*, on the initial conditions of the system (Thompson and Stewart, 1986; Prasad *et al.*, 2005). We consider one of the example from Prasad *et al.* (2005), where the dynamical hysteresis in coupled oscillators have been observed in terms of stability of the system using Lyapunov exponents in a wide range of parameter space. It is conceptually difficult to estimate the Lyapunov exponent for a small and noisy data set. In order to see the hysteresis region using the permutation entropy, we consider Rössler-type (Gaspard and Nicolis, 1983) coupled oscillators, as shown schematically in Figure 1. The model equations for this system are

$$\begin{aligned}\frac{dx_i(t)}{dt} &= -w_i y_i - z_i + F_i(\epsilon, x_i, x_j), \\ \frac{dy_i(t)}{dt} &= w_i x_i + a_i y_i, \\ \frac{dz_i(t)}{dt} &= \beta_i x_i + z_i(x_i - y_i),\end{aligned}\tag{3}$$

where $i, j=1, 2, 3, 4$ (number of oscillators= 4), $w_1 = 1.005, w_2 = w_3 = w_4 = 0.995, a_i = 0.38, \beta_i = 0.3$, and $\gamma_i = 4.5$. At these set of parameters all the individual systems show chaotic oscillations (Prasad *et al.*, 2005). The coupling functions are $F_1 = \epsilon(x_2 + x_3 + x_4 - 3x_1), F_2 = \epsilon(x_1 - x_2), F_3 = \epsilon(x_1 - x - 3)$, and $F_4 = \epsilon(x_1 - x_4)$ while ϵ is the coupling parameter. In our numerical calculation, we used the fourth-order Runge-Kutta integrator with integration time step 0.01.

Prasad *et al.* (2005) have shown the hysteresis behavior in the largest Lyapunov exponent with respect to the coupling parameter ϵ , and predicted the coexistence of more than one state of different type of stability in the hysteresis region. In

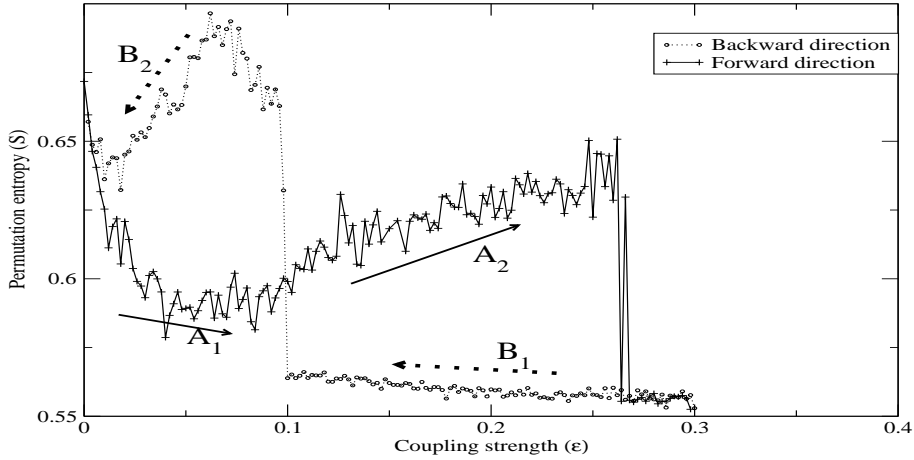


Figure 2. Permutation entropy (S) for increasing (solid line) and decreasing (dotted line) coupling strengths (ϵ) for the coupled system represented by Equation (3). Arrows with symbols A and B indicate the paths for increasing and decreasing coupling strengths, respectively.

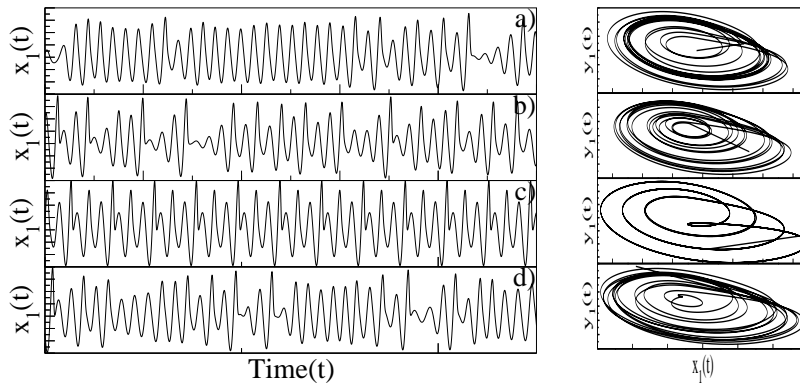


Figure 3. The time series $x_1(t)$ in regions (a) $A_1(\epsilon = 0.05)$, (b) $A_2(\epsilon = 0.20)$, (c) $B_2(\epsilon = 0.20)$, and (d) $B_1(\epsilon = 0.05)$, respectively of Figure 2. The right-hand-side panel shows the corresponding projection of trajectories into the $x - y$ plane.

order to check the presence of hysteresis and dynamical changes in terms of permutation entropy S , we consider the x -component of the time series of the first oscillator. We take embedding dimension $m = 5$ (although higher values of m gives similar results) and sampling time $\tau = 300$ (first minima of the auto-correlation function). 750 data points are used to calculate S . Figure 2 shows a plot of S as a function of increasing and decreasing coupling strengths ϵ . The arrows show the corresponding increasing and decreasing coupling strengths. The hysteresis region is visible for different values of ϵ . Figures 3(a–d) show the time series $x_1(t)$ and the projection of the first oscillator in the $x - y$ plane at regions

corresponding to $A_1(\epsilon = 0.05)$, $A_2(\epsilon = 0.2)$, $B_2(\epsilon = 0.2)$, and $B_1(\epsilon = 0.05)$ of Figure 2. Although the trajectories look similar, the corresponding permutation entropy (S) shows that they are dynamically different. Importantly, the permutation entropy captures the hysteresis loop as shown with Lyapunov exponents in Prasad *et al.* (2005).

4. Permutation Entropy of the Solar Wind Data

We use hourly averaged solar wind velocity data at a distance of 1 AU obtained from the Solar Wind Ion Composition Spectrometer (SWICS) on ACE (<http://www.srl.caltech.edu/ACE/ASC/level2/>). This data set corresponds to the years 1998 to 2010. Since the data are not continuous we split the data set into 18 continuous time series to cover most of the solar cycle 23. The details of the time series used are given in Table 1. In addition, Table 1 (last column) contains the corresponding sunspot numbers for each time series taken from <http://sidc.oma.be/sunspot-data/>. Figure 4 shows the solar activity during activity cycle 23. The position of serial numbers corresponding to the solar wind data sets, is shown on the smoothed monthly averaged sunspot index curve.

Table 1. Hourly averaged solar wind velocity data measured by the ACE spacecraft in the years 1998 to 2010: Initial time (T_i), Number of Data points (N), and Sunspot numbers (SSN). Sunspot numbers are from <http://sidc.oma.be/sunspot-data/>.

| S.No. | T_i | N | Sunspot number (SSN) |
|-------|---------|------|----------------------|
| 1 | 1998.25 | 1665 | 54 |
| 2 | 1998.71 | 1314 | 69 |
| 3 | 1998.91 | 789 | 75 |
| 4 | 1999.11 | 1927 | 84 |
| 5 | 1999.41 | 2716 | 92 |
| 6 | 1999.73 | 1139 | 104 |
| 7 | 1999.94 | 1404 | 111 |
| 8 | 2000.15 | 3075 | 117 |
| 9 | 2000.88 | 1580 | 113 |
| 10 | 2001.40 | 1315 | 110 |
| 11 | 2002.03 | 3329 | 113 |
| 12 | 2002.41 | 3417 | 107 |
| 13 | 2003.03 | 789 | 81 |
| 14 | 2003.24 | 1840 | 72 |
| 15 | 2003.90 | 2633 | 54 |
| 16 | 2005.33 | 2541 | 30 |
| 17 | 2006.45 | 2278 | 16 |
| 18 | 2008.39 | 2108 | 3.5 |

We calculate the normalized permutation entropy S for all 18 time series using embedding dimension $m = 5$ and window length of 750 points. We use six overlapping windows and then calculated the average value of S . The standard deviation in S is given by

$$\sigma = \sqrt{\frac{\sum_{i=1}^n (S_i - S_{\text{avg}})^2}{n}}, \quad (4)$$

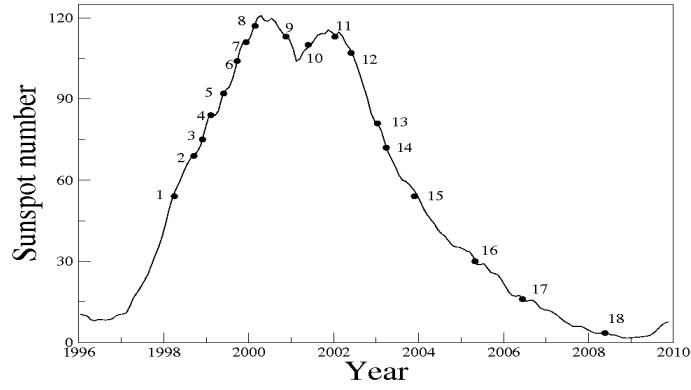


Figure 4. Smoothed monthly sunspot number from 1996 to 2010. Serial numbers 1 – 18 correspond to the solar wind data sets given in Table 1.

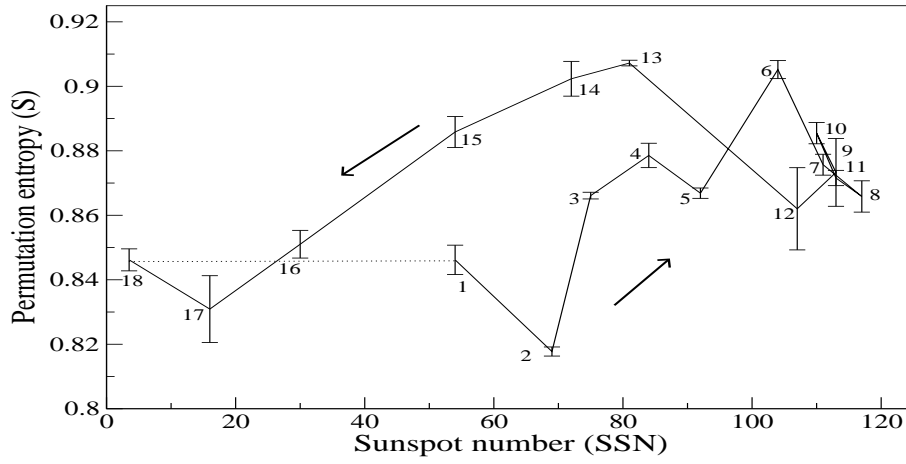


Figure 5. Permutation entropy vs. sunspot number for solar wind time series with 1σ error bars. The dotted line is the possible connection between 1 and 18. Arrows show the direction of time.

where n is the number of overlapping windows, S_{avg} is the average permutation entropy of n windows, and σ estimates the statistical uncertainties in the average. Figure 5 shows the plot of S_{avg} of solar wind time series vs. sunspot number corresponding to the time of solar wind observation. The error bars are estimates of the statistical uncertainties in these averages.

It is noticeable that the path followed by the permutation entropy of the solar wind data in the increasing phase of the solar activity cycle is different from that of the decreasing phase, *i.e.*, a hysteresis phenomenon is present. It shows that although sunspot data set is almost symmetric around the peak of the solar activity cycle yet permutation entropy of solar wind data follows different paths in increasing and decreasing phases of the solar activity cycle.

5. Conclusions

The long term sunspot time series shows an average cycle length of 11 years. Although nearly periodic, the period as well as amplitude of the cycle varies irregularly. Apart from the sunspot data, the intrinsic irregularity of the solar cycle is seen in other observable variables like surface flows, solar irradiance (solar constant), the solar wind, and so on. The Maunder Minimum and several ancient periods from solar proxy-data suggest that the Sun exhibits quasi-periodic or intermittent behavior (Feminella and Storini, 1997). Owing to changes in magnetic activity, many aspects of the solar wind change over a solar cycle, including the speed, the density, the dynamic pressure, the composition, and the temperature (Richardson and Kasper, 2008).

In this paper, we present the analysis of solar wind velocity data during the solar activity cycle 23. We obtained 18 different time series of hourly averaged solar wind velocity, measured by ACE spacecraft at 1 A.U. To quantify the randomness of these time series, we use a robust, conceptually simple and computationally efficient measure called permutation entropy. A smaller value of permutation entropy indicates a more regular time series. We observe that as the solar cycle 23 progresses towards maximum, the permutation entropy increases, saturates around the peak of activity and then decreases as the activity of cycle 23 subsides. We also note (Figure. 5) that the value of permutation entropy follows different paths in the ascending and descending phases of the solar activity cycle. In addition, while the ascent is fluctuating, the descent is smooth. This hysteresis phenomenon shows the multistability in the dynamics of solar wind, over the solar activity cycle. The behavior is similar to the one observed for hysteresis phenomenon of other solar indices (Bachmann and White, 1994; Jiménez-Reyes *et al.*, 1998; Özgüç and Ataç, 2001) and confirms (*cf.* Consolini, Tozzi, and de Michelis, 2009) that spatio-temporal or dynamical complexity is an intrinsic property of the solar cycle.

Acknowledgements The authors thank the ACE Science Center and instrument teams for making available the ACE data used here. VS and AP thank CSIR for SRF and DST Govt. of India for financial supports respectively.

References

- Alfsen, K.H., Frøyland, J.: 1985, *Phys. Scr.* **31**, 15.
 Bachmann, K.T., White, O.R.: 1994, *Solar Phys.* **150**, 347.
 Bandt, C., Pompe, B.: 2002, *Phys. Rev. Lett.* **88**, 174101.
 Bertotti, G.: 1998, *Hysteresis in Magnetism: For Physicists, Materials Scientists, and Engineers*, Academic Press, New York. 31.
 Cao, Y., Tung, W., Gao, J.B., Protopopescu, V.A., Hively, L.M.: 2004, *Phys. Rev. E* **70**, 046217.
 Consolini, G., Tozzi, R., de Michelis, P.: 2009, *Astron. Astrophys.* **506**, 1381.
 Feminella, F., Storini, M.: 1997, *Astron. Astrophys.* **322**, 311.
 Gaspard, P., Nicolis, G.: 1983, *J. Stat. Phys.* **31**, 499.
 Gupta, K., Prasad, A., Saikia, I., Singh, H.P.: 2008, *Planet. Space Sci.* **56**, 550.
 Guyer, R.A., TenCate, J., Johnson, P.: 1999, *Phys. Rev. Lett.* **82**, 3280.
 Hapgood, M.A., Lockwood, M., Bowe, G.A., Wills, D.M., Tulunay, Y.K.: 1991, *Planet. Space Sci.* **39**, 411.

- Jiménez-Reyes, S.J., Régulo, C., Pallé, P.L., Roca Cortés, T.: 1998, *Astron. Astrophys.* **329**, 1119.
- Kantz, H., Schreiber, T.: 2004, *Nonlinear Time Series Analysis*, Cambridge University Press, Cambridge, 10.
- Katzgraber, H.G., Pázmándi, F., Pike, C.R., Liu, K., Scalettar, R.T., Verosub, K.L., Zimányi, G.T.: 2002, *Phys. Rev. Lett.* **89**, 257202.
- Macek, W.M., Obojska, L.: 1997, *Chaos Solitons Fractals* **8**, 1601.
- Macek, W.M.: 1998, *Physica D: Nonlinear Phenomena* **122**, 254.
- Macek, W.M., Obojska, L.: 1998, *Chaos Solitons Fractals* **9**, 221.
- Macek, W.M., Redaelli, S.: 2000, *Phys. Rev. E* **62**, 6496.
- McComas, D.J., Gosling, J.T., Skoug, R.M.: 2000, *Geophys. Res. Lett.* **27**, 2437.
- Milano, L.J., Dasso, S., Matthaeus, W.H., Smith, C.W.: 2004, *Phys. Rev. Lett.* **93**, 155005.
- Moreno-Insertis, F., Solanki, S.K.: 2000, *Mon. Not. Roy. Astron. Soc.* **313**, 411.
- Özgüç, A., Ataç, T.: 2001, In: Brekke, P., Fleck, B., Gurman, J. B. (eds.), *Recent Insights into the Physics of the Sun and Heliosphere: Highlights from SOHO and Other Space Missions*, *IAU Symp.* **203**, 125.
- Packard, N.H., Crutchfield, J.P., Farmer, J.D., Shaw, R.S.: 1980, *Phys. Rev. Lett.* **45**, 712.
- Prasad, A., Iasemidis, L.D., Sabesan, S., Tsakalis, K.: 2005, *Pramana* **64**, 513.
- Redaelli, S., Macek, W.M.: 2001, *Planet. Space Sci.* **49**, 1211.
- Richardson, J.D., Kasper, J.C.: 2008, *J. Atmos. Solar-Terr. Phys.* **70**, 219.
- Rosso, O.A., Larrondo, H.A., Martin, M.T., Plastino, A., Fuentes, M.A.: 2007, *Phys. Rev. Lett.* **99**, 154102.
- Schwenn, R.: 2007, In: Baker, D. N., Klecker, B., Schwartz, S. J., Schwenn, R., von Steiger, R. (eds.), *Solar Dynamics and its Effects on the Heliosphere and Earth*, Springer, New York, 51.
- Suyal, V., Prasad, A., Singh, H.P.: 2011, Submitted to *Planet Space Sci.*
- Thompson, J.M.T., Stewart, H.B.: 1986, *Nonlinear Dynamics and Chaos*, John Wiley and Sons, New York. 123.
- Tripathy, S., Kumar, B., Jain, K., Bhatnagar, A.: 2000, *J. Astrophys. Astron.* **21**, 357.
- Zharkov, G.: 2002, *J. Exp. Theor. Phys.* **95**, 517.

